DAEHAN HWAHAK HWOEJEE
(Journal of the Korean Chemical Society)
Vol. 21, No. 5, 1977
Printed in Republic oforea

소성변형의 분자론 (제2보). 응용

金 昌 弘·李 泰 圭
한국과학원 화학 및 화학공학과
(1977. 5. 20 접수)

Molecular Theory of Plastic Deformation (II). Applications

Chang Hong Kim and **Taikyue Ree**
Korea Advanced Institute of Science, Seoul, Korea
(Received May 20, 1977)

요 약. 소성변형에 대한 저자들의 이론(제 1 보)[1]을 요업재료, 금속, 합금 및 단결정들에 적용하였다. 그 결과 다중 결정에서는 dislocation 운동과 grain boundary 운동이 실험조건에 따라 함께 또는 분리되어 나타나는 반면 단결정에서는 dislocation 운동만 나타났다. 유동식에 나타나는 파라미터 (α_{d1}, $1/\beta_{d1}$)와 (α_{gj}/X_{gj}, $1/\beta_{gj}$) (j=1 혹은 2) 및 활성화엔탈피 $\Delta H_{k1}^{\pm}$ ($k=d$ 혹은 g)를 구하여 예측한 소성변형은 실험과 잘 일치함을 보았다. 여기서 첨자 $d1$는 첫번째의 dislocation 유동단위, gj는 j 번째 grain boundary 유동단위를 나타낸다. 활성화엔탈피에 대하여 $\Delta H_{d1}^{\pm}$는 bulk의 자체확산에 대한 활성화엔탈피와 일치하고 $\Delta H_{g1}^{\pm}$는 grain boundary 자체확산에 대한 활성화엔탈피와 일치하였다. 이 사실은 저자들의 이론의 정당성을 보이고 있다.

ABSTRACT. The authors' theory developed in the preceding Paper 1[1] was applied to plastic deformation of ceramics, metals, alloys and single crystals. For polycrystalline substances, the flow mechanisms due to dislocation movement and grain boundary movement appear together or separately according to the experimental conditions whereas for single crystals, only the mechanism of dislocation movement appears. The parameters appearing in the flow equations (α_{d1}, $1/\beta_{d1}$) and (α_{gj}/X_{gj}, $1/\beta_{gj}$) (j=1 or 2), and the activation enthalpies $\Delta H_{k1}^{\pm}$ ($k=d$ or g) were determined and tabulated. Here, the subscript $d1$ indicates the first kind of dislocation flow units and gj expresses the jth kind of grain boundary flow units.

The predictions of the theory were compared with experiment with good agreement. Concerning the activation enthalpies, it was found that $\Delta H_{d1}^{\pm} > \Delta H_{g1}^{\pm}$ and that the former agrees with the activation enthalpy for bulk self-diffusion whereas the latter agrees with the activation enthalpy for grain boundary self-diffusion. These facts support the adequacy of the authors' theory which is considered as a generalized theory of plastic deformation.

INTRODUCTION

In the preceding Paper I,[1] we derived general equations for total stress f and shear rate $\dot{s}$,

$$f=f_d=\sum_i^n X_{di}f_{di} = f_g=\sum_j X_{gj}f_{gj} \quad (1)$$

$$\dot{s}=\frac{1}{\beta_{di}}\sinh\left(\frac{\alpha_{di}}{X_{di}}X_{di}f_{di}\right)+\frac{1}{\beta_{gj}}\sinh\left(\frac{\alpha_{gj}}{X_{gj}}X_{gj}f_{gj}\right) \quad (2)$$

where f_d and f_g are the stress on a dislocation shear plane and on a grain boundary shear plane, respectively; f_{kn} is the stress acting on flow units of kind n (i or j) of flow type k(d or g); X_{kn} is the fraction of area on a shear surface occupied by flow units of kind n of type k; $\alpha_{kn}=(\lambda\lambda_2\lambda_3)_{kn}/(2kT)$; $\beta_{kn}=1/[(\lambda/\lambda_1)2k']_{kn}$; k' is the rate constant for the flow process when there is no stress applied; λ_1, λ_2, λ_3, and λ are the molecular parameters in Eyring's viscosity formula;[2] and the subscript kn outside the parentheses indicates that the inside quantities belong to flow units kn($kn=di$ or gj). By various combination of flow units kn, many kinds of plastic deformation patterns would be produced from Eqs. (1) and (2). In Paper 1, the four cases which are important in practice were considered. In this paper, the flow equations developed in Paper 1 will be applied to experimental deformation data, and the results will be discussed.

SYNOPSIS OF THE THEORY

It is appropriate in the beginning to make a brief review on the results in Paper 1.

The simplest case is Case 1, where a single kind of flow units is acting. The creep equations for dislocation movement are

$$f=f_d=X_{d1}f_{d1}=f_{d1},$$

$$\dot{s}=\frac{1}{\beta_{d1}}\sinh\left(\frac{\alpha_{d1}}{X_{d1}}X_{d1}f_{d1}\right)=\frac{1}{\beta_{d1}}\sinh(\alpha_{d1}f) \quad (3a)$$

And similar equations hold for grain boundary movement:

$$f=f_g=X_{g1}f_{g1}=f_{g1},$$

$$\dot{s}=\frac{1}{\beta_{g1}}\sinh\left(\frac{\alpha_{g1}}{X_{g1}}X_{g1}f_{g1}\right)=\frac{1}{\beta_{g1}}\sinh(\alpha_{g1}f) \quad (3b)$$

The next case of interest is Case 2 where all the flow units of a given type are connected in parallel. The corresponding flow equations for dislocation movement are

$$f=\sum_i^m X_{di}f_{di}$$
$$\dot{s}=\frac{1}{\beta_{di}}\sinh\left(\frac{\alpha_{di}}{X_{di}}X_{di}f_{di}\right) \quad (4a)$$

and for grain boundary movement, the equations are

$$f=\sum_i^m X_{gj}f_{gj}$$
$$\dot{s}=\frac{1}{\beta_{gj}}\sinh\left(\frac{\alpha_{gj}}{X_{gj}}X_{gj}f_{gj}\right) \quad (4b)$$

When $m=2$, the total stress f is calculated by

$$f=\frac{X_{k1}}{\alpha_{k1}}\sinh^{-1}(\beta_{k1}\dot{s})+\frac{X_{k2}}{\alpha_{k2}}\sinh^{-1}(\beta_{k2}\dot{s}) \quad (4c)$$

which is derived from Eqs. (4a) and (4b), k being equal to d or g.

Case 3 deals with the case where a single kind of dislocation flow units and a sigle kind of grain boundary flow units are connected in series. The flow equations are

$$f=f_d=X_{d1}f_{d1}=f_{d1}=f_g=X_{g1}f_{g1}=f_{g1} \quad (5)$$

and

$$\dot{s}=\frac{1}{\beta_{d1}}\sinh(\alpha_{d1}f)+\frac{1}{\beta_{g1}}\sinh(\alpha_{g1}f) \quad (6)$$

The most complicated case is Case 4 where a single kind of dislocation flow units is connected with a system in which two kinds of grain boundary flow units are connected in parallel. The corresponding creep equations are

$$f=f_d=X_{d1}f_{d1}=f_{d1}=f_g=X_{g1}f_{g1}+X_{g2}f_{g2} \quad (7)$$

and

$$\dot{s}=\frac{1}{\beta_{d1}}\sinh(\alpha_{d1}f)+\frac{1}{\beta_{g2}}\sinh\left(\frac{\alpha_{g2}}{X_{g2}}X_{g2}f_{g2}\right) \quad (8)$$

where $X_{g2}f_{g2}$ can be calculated from the relation

$$\frac{\sinh\left[\frac{\alpha_{g1}}{X_{g1}}(f-X_{g2}f_{g2})\right]}{\sinh\left(\frac{\alpha_{g2}}{X_{g2}}X_{g2}f_{g2}\right)}=\frac{\beta_{g1}}{\beta_{g2}}\equiv C \quad (9)$$

In order to test our theory, it will be necessary to determine the parameters appearing in Eqs. (3), (4), (6) and (8), and to calculate $\dot{s}$ from these equations. The predicted $\dot{s}$ will be compared with experiment, the good agreement being the justification for our theory. In the present paper, all the parameters were determined by using the method described in Paper 1.

APPLICATIONS

1. Magnesia. Hensler *et al.*[3] studied the compressive creep behaviour of cylindrical MgO polycrystals (10 mm diameter, 25 mm length, 13 to 68μ grain size). The experimental data of f *vs.* $-\ln \dot{s}$ are shown in *Fig.* 1.

Our analysis showed that the pattern of the curve at 1400°C in *Fig.* 1 belongs to Case 3 which is the series connection of disln. 1 and GB1, where disln. 1 and GB1 denote dislocation flow unit 1 and grain boundary flow unit 1, respectively. The parameters α_{k1} and $1/\beta_{k1}$ ($k=d$ or g) determined by the method stated in Paper 1 are tabulated in *Table* 1.

The theoretical curves were calculated from Eq. (6) by using the parameters in *Table* 1. It is worthy of note that the theoretical curves for 1300°C and 1500°C in *Fig.* 1 were obtained from the paprameters of α_{k1} and $1/\beta_{k1}$ in *Table* 1 at 1400°C and from ΔH_{k1}^{*} ($k=d$ or g) in *Table* 5. The value of ΔH_{k1}^{*} was determined by using the method detailed in Paper 1. The experimental data are in good agreement with the theoretical curves. This fact indicates the adequacy of the Hahn-Ree-Eyring theory.[4]

Hensler *et al.*[3] observed no structural change and no increase is porosity with the creep deformation, and noted especially that the grains did not change measurably in the length-to-width ratio with overall compressive deformation of the specimen as large as 40%. Thus

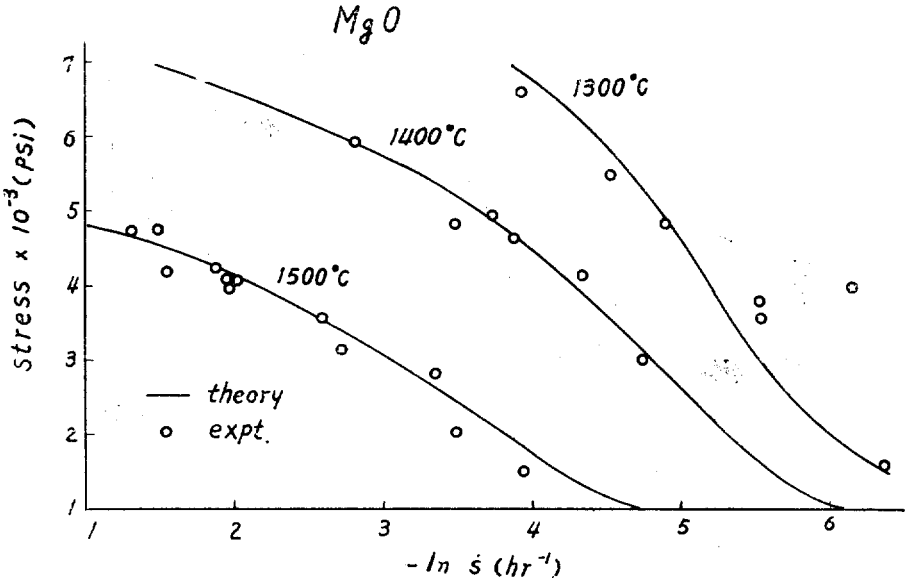

Fig. 1. Creep curves for MgO polycrystals. Curves for 1300°C and 1500°C were obtained from the flow parameters at 1400°C (*Table* 1) and ΔH_{k1}^{*} ($k=d$ or g) (*Table* 5).

Table 1. Flow parameters for polycrystals of ceramics.

Sample	α_{d1} (psi)$^{-1}$	α_{g1} (psi)$^{-1}$	$1/\beta_{d1}$	$1/\beta_{g1}$	Temp. (°C)	*Figure*
MgO(13~68μ)	1.4×10^{-3}	1.75×10^{-4}	3.88×10^{-4} hr^{-1a}	2.06×10^{-2} hr^{-1a}	1500	*Fig.* 1
MgO(13~68μ)	1.4×10^{-3}	1.75×10^{-4}	2.53×10^{-5} hr^{-1}	1.26×10^{-2} hr^{-1}	1400	*Fig.* 1
MgO(13~68μ)	1.4×10^{-3}	1.7×10^{-4}	1.17×10^{-6} hr^{-1a}	6.95×10^{-3} hr^{-1a}	1300	*Fig.* 1
YSZ (17μ)	8.47×10^{-4}	3.79×10^{-4}	2.64×10^{-6} hr^{-1}	5.56×10^{-5} hr^{-1}	1485	Fig. 2
SSZ (1μ)		2.21×10^{-4b} 1.64×10^{-3c}		3.18×10^{-1} hr^{-1} 4.76×10^{-3} hr^{-1d}	1378	*Fig.* 2
Al_2O_3 (50μ)	4.95×10^{-2}	3.44×10^{-3b} 1.19×10^{-2c}	1.49×10^{-29} hr^{-1}	1.00×10^{-2} hr^{-1} 6.02×10^{-7} hr^{-1d}	1800	*Fig.* 3
Al_2O_3 (34μ)		3.15×10^{-4}		1.37×10^{14} hr^{-1d}	1800	*Fig.* 3[e]
Al_2O_3 (7μ)	6.00×10^{-4}	4.20×10^{-5}	2.72×10^{-11} min^{-1}	1.01×10^{-3} min^{-1}	1500	*Fig.* 3
Al_2O_3 (7μ)	6.00×10^{-4}	4.20×10^{-5}	3.07×10^{-1} min^{-1a}	5.67×10^{-3} min^{-1a}	1600	*Fig.* 3

[a]Values obtained by substituting $\Delta H_{i1}^{\ddagger}$ ($k=d$ or g) (*Table* 5) to Eqs. (15a) and (15b) of reference 1. [b]This valus represents α_{g1}/X_{g1}. [c] This value represents α_{g2}/X_{g2}, [d]This value represents $1/\beta_{g2}$. [e]Parameters obtained from the curve f *vs.* $-\ln Z$ where $Z=\dot{s}\exp(\Delta H^{\ddagger}/RT)$.

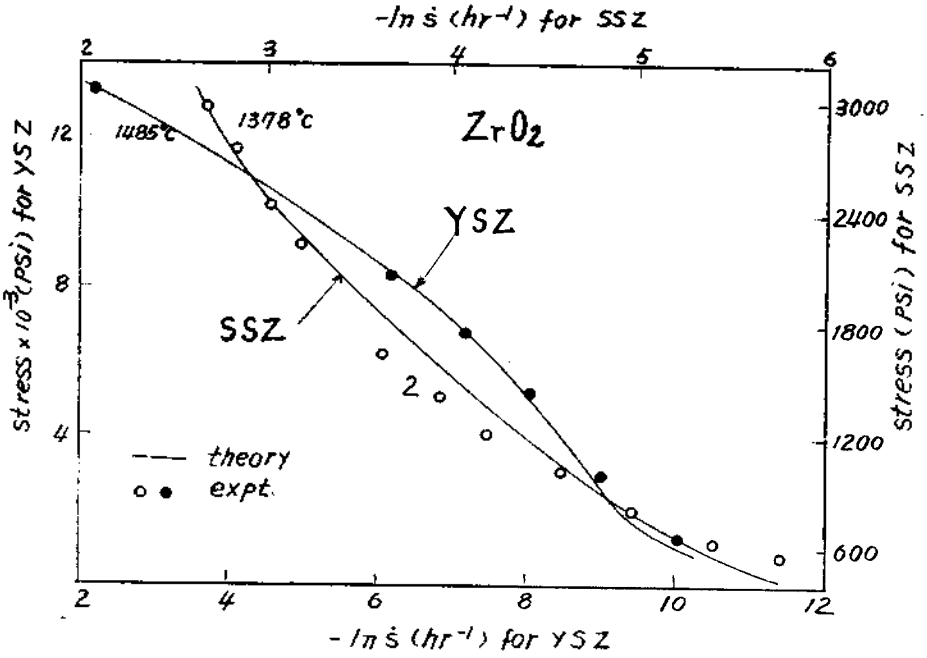

Fig. 2. Creep curves for ZrO_2 polycrystals: Cruve 1, yttria stabilized zirconia (YSZ). Curve 2, scandia stabilized zirconia (SSZ).

Hensler concluded that creep in MgO appears to occur by extensive grain boundary sliding. According to our result, however, the creep deformation occurs not only by the grain boundary movement, but also by the dislocation movement.

2. Zirconia. Evans *et al.*[5] observed the compressive creep of scandia-stabilized zirconia (SSZ) and yttria-stabilized zirconia (YSZ). The specimens were cylinders (0.2″ diameter, 0.4″

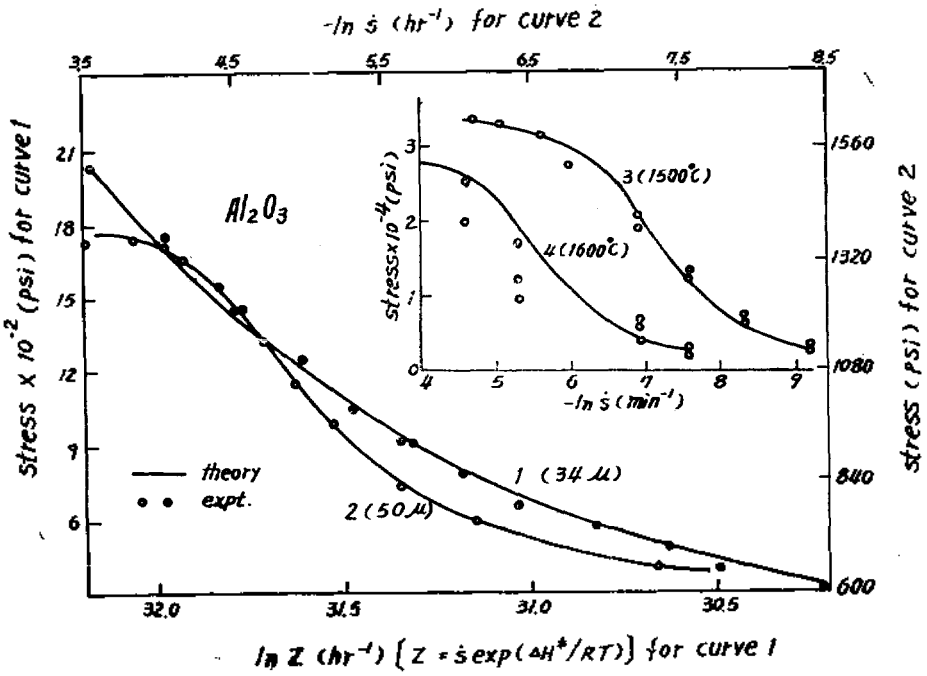

Fig. 3. Creep curves for Al_2O_3 polycrystals of different grain sizes and temperatures. Curve 1, grain size 34μ, at 1800°C. Curve 2, 50μ, at 1800°C. Curve 3. 7μ, at 1500°C. Curve 4, 7μ, at 1600°C. Curve 4 (1600°C) was obtained from the flow parameters at 1500°C (*Table* 1) and ΔH_k^* ($k=d$ or g) (*Table* 5).

length), and SSZ was 1μ in grain size containing 6 mole % Sc_2O_3, and YSZ was 17μ in grain size containing 6 mole % Y_2O_3.

The creep data for these specimens (*Fig.* 2) were analysed, and the necessary parameters were obtained by the method described in Paper 1, and are shown in *Table* 1. In *Fig.* 2, YSZ showed the deformation belonging to Case 3 (the series-connection of GB1 and disln. 1 flow units). The theoretical curve of f *vs.* $-\ln \dot{s}$ was obtained by introducing α_{k1} and $1/\beta_{k1}$ ($k=d$ or g) in *Table* 1 to Eq. (6). One notes that the experimental data well agree with the theoretical cueve. On the other hand, the SSZ showed the deformation belonging to Case 2 (the parallel connection of GB1 and GB2 flow units). The deformation of SSZ appeared in the low stress region, where YSZ deforms predominantly by the grain boundary movement. Because of the low stress region, SSZ showed only the deformation due to the grain boundary flow units. The theoretical curve for SSZ was calculated from Eq. (4c) by using α_{gj}/X_{gj} and $1/\beta_{gj}$ ($j=$ 1 or 2) in *Table* 1.

Microstructural observation showed that no change in grain size occurred before and after creep deformation, and that the pores on boundaries moved toward the stress axis for both YSZ and SSZ.[5]

3. Alumina. Warshaw and Norton[6] examined the steady-state creep behavior of polycrystalline Al_2O_3 at 1800°C over a range of stress from 100 to 2000 psi using the four-point transverse bending method. The specimen was a bar one face of which was $3/64'' \times 1''$. Curve 2 in *Fig.* 3 is for polycrystalline Al_2O_3 (above 50μ in grain size), and corresponds to Case 4. The theoretical curve 2 was obtained by introducing the parameters α_{d1}, $1/\beta_{d1}$, α_{g2}/X_{g2}, $1/\beta_{g2}$ (*Table* 1) and $X_{g2}f_{g2}$ [calculated from Eq.

(9)] to Eq. (8). The agreement between experiment and theory is very good. Curve 1 is the result for the polycrystalline Al_2O_3 (34μ grain size) over a low stress region, and it exhibits a pattern of deformation different from the alumina sample mentioned above. Curve 1 corresponds to Case 1 (a single type of grain boundary flow units); the theoretical curve was obtained by introducing the parameters α_{g1} and $1/\beta_{g1}$ in *Table* 1 into Eq. (3b).

Microstructural observation showed that the grain structure for coarse-grained alumina (50μ to 100μ) was not so well defined as in the case of the fine-grained structure, i.e., there were regions of abnormal grain growth in the structure, and the grains were columnar rather than quasi-spherical. But no change was observed in grain shape and grain size before and after creep deformation for the coarse grain alumina as well as for all the finely-grained alumina (3, 7, 13, 34μ).[6] Curves 1 and 2 in *Fig.* 3 are quite different in the deformation patterns although the experiments were conducted at about same stress levels. The different pattern is considered to be due to the large difference in the grain structures between coarse-and fine-grained alumina.

Folweiler[7] also examined the steady-state creep behavior of the pore-free, fine-grained alumina of various grain size prepared in the same way as in Warshaw's method.[6] This author studied at temperatures from 1500 to 1800°C over a range of stresses from 1000 to 33,000 psi by using three-point transverse bending method. The specimen size was approximately $0.1'' \times 0.15'' \times 2''$. The experimental data are plotted in *Fig.* 3 (see curves 3 and 4), and the parameters α_{k1} and $1/\beta_{k1}$ ($k=d$ or g) obtained from these data are shown in *Table* 1. This case belongs to Case 3 (series connection of disln. 1 and GB1 flow units). The theoretical curves 3 and 4 in *Fig.* 3 is obtained by introducing the parameters in *Table* 1 to Eq. (6) describing Case 3. Previously, we found that curve 1 in *Fig.* 3, which was obtained for polycrystalline Al_2O_2 (34 μ grain size), belonged to Case 1 (a single kind of GB1 flow units) whereas the curves 3 and 4, which was obtained for polycrystalline Al_2O_3 (7 μ grain size), belong to Case 3. The main reason for this difference is in the stress levels since the experimental data of curve 3 and 4 in *Fig.* 3 were obtained under stresses ranging from low to high levels. Thus, the data of curve 3 and 4 showed the movements due to dislocation flow units as well as the grain boundary flow units whereas curve 1 showed only the grain boundary movement since it was obtained at such low stress levels at which only grain boundary movement is possible.

The theoretical curve 4 (1600°C) in *Fig.* 3 was obtained from the parameters α_{k1}, $1/\beta_{k1}$ ($k=d$ or g) at 1500°C (*Table* 1) and ΔH_{k1}^{*} ($k=d$ or g) (*Table* 5). Considering the large relative error of the experimental data of 1600 °C, the theory seems to be in satisfactory agreement with experiment.

Microstructural observations[7] showed that there was a strong tendency for voids to occur on boundaries perpendicular to the principal tensile stress, and that the small voids grew up to larger ones along the grain boundaries. Grain rotation and grain boundary sliding was also observed.

4. Commercial 7075 Aluminum. Commercial 7075 aluminum is an Al-Zn-Mg-Cu alloy the composition of which is: Al(base), Zn(5.84%), Mg(2.61%), Cu(1.6%), trace of Si, Fe, Mn, Ti, Cr, Ni and Zr. Embury *et al.*[8] studied the tensile deformation behavior of this alloy at various temperatures. The authors confirmed by observing the microstructures that at 100°C and

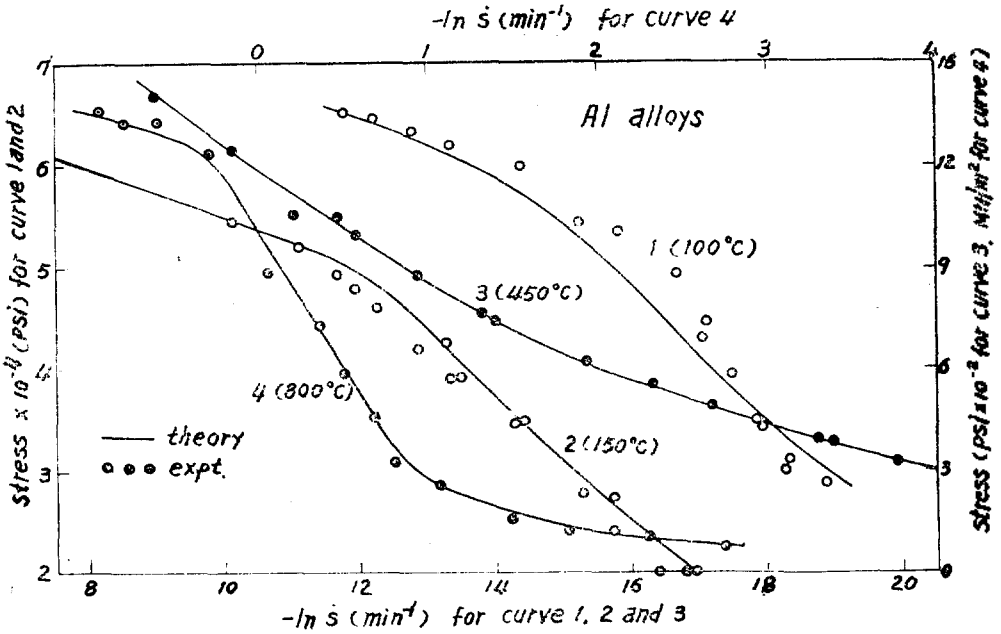

Fig. 4. Creep curves for Al-alloys. Curve 1, 2 and 3 are for commercial 7075 aluminum at different temperatures, and curve 4 for Al-bronze at 800°C. Curve 1 (100°C) was obtained from the flow parameters at 150°C (*Table* 2) and ΔH_{k1}^* ($k=d$ or g) (*Table* 5).

Table 2. Flow parameters for the polycrystals of metals and alloys.

Sample	α_{d1}	α_{g1}	$1/\beta_{d1}$	$1/\beta_{g1}$	Temp (°C)	*Figure*
7075 Al (Al-Zn-Mg-Cu)	4.69×10^{-4} (psi)$^{-1}$	1.54×10^{-4} (psi)$^{-1}$	5.19×10^{-19} min^{-1}[a]	1.19×10^{-10} min^{-1}[a]	100	*Fig.* 4
(Al-Zn-Mg-Cu)	4.69×10^{-4} (psi)$^{-1}$	1.5×10^{-4} (psi)$^{-1}$	3.59×10^{-16} min^{-1}	4.65×10^{-9} min^{-1}	150	*Fig.* 4
(Al-Zn-Mg-Cu)		1.33×10^{-2} (psi)$^{-1}$[b] 1.67×10^{-2} (psi)$^{-1}$[c]		8.77×10^{-7} min^{-1} 1.81×10^{-11} min^{-1}[d]	450	*Fig.* 4
Al-bronze (Cu base-Al-Fe)	2.00 (MN/m^2)$^{-1}$	3.49×10^{-1} (MN/m^2)$^{-1}$[b] 4.51×10^{0} (MN/m^2)$^{-1}$[c]	1.84×10^{-11} min^{-1}	1.65×10^{-1} min^{-1} 7.40×10^{-5} min^{-1}[d]	800	*Fig.* 4
Zr (50μ)	2.50×10^{-3} (psi)$^{-1}$	4.61×10^{-4} (psi)$^{-1}$	2.36×10^{-6} hr^{-1}	1.22×10^{-4} hr^{-1}	567	*Fig.* 5
Zircaloy-2 (10μ)	9.00×10^{-4} (psi)$^{-1}$	2.79×10^{-5} (psi)$^{-1}$	2.53×10^{-6} hr^{-1}	8.57×10^{-4} hr^{-1}	551	*Fig.* 5

[a]Values obtained by introducing ΔH_{k1}^* ($k=d$ or g) (*Table* 5) to Eqs. (15a) and (15b) in reference 1; [b]This value represents α_{g1}/X_{g1}; [c]This value represents α_{g2}/X_{g2}; [d]This value represents $1/\beta_{g2}$.

150°C, the deformation occurs by both dislocation and grain boundary movement and that simple nets of dislocations have developed within the original subgrains. They also found that at 450°C, the contribution of grain boundary sliding was predominant.

The experimental data (f and $-\ln\dot{s}$) are plotted in *Fig.* 4 (see curve 1, 2 and 3). The parameters for this alloy are given in *Table* 2, from which theoretical curves 1 (100°C), 2 (150 °C), and 3 (450°C) were calculated, and shown in *Fig.* 4. According to *Fig.* 4, curve 1

(100°C) and 2 (150°C) belong to Case 3, but curve 3 (450°C) belongs to Case 2. Here curve 1 (100°C) is a predicted one from the parameters at 150°C and ΔH_{fl}^{*} ($k=d$ or g) in *Table* 5, and one notes that the agreement with experiment is satisfactory. The reason that the creep behavior of curve 3 (450°C) is different from that of curve 1 and 2 is considered to be responsible to the phase transformation of the GP zone to the η phase which occurs at 450°C, and also to the low stress level where the experiment was performed. The theoretical curve 3 (450°C) was calculated from Eq. (4c) by using the parameters α_{gj}/X_{gj} and $1/\beta_{gj}$ ($j=1$ or 2) on *Table* 2.

5. **Al-Bronze.** Dunlop *et al.*[9] investigated the microstructure of micrograins of Al-bronze (CDA alloy 619, Cu base, Al 9.5%, Fe 4.0%) after deformation over various range of strain rates at 800°C. The results showed that in the low strain rate range, clumps of grains slide together as units on sliding interface. After deformation in this low strain-rate range there was no evidence for dislocation motion within the grains. With increasing strain-rate, however, evidence for dislocation motion steadily increased whereas the tendency for grain sliding deminished.

The experimental data are shown in *Fig.* 4 (curve 4). The pattern of curve 4 belongs to Case 4. Curve 4 is the theoretical curve obtained by introducing the parameters of α_{d1}, $1/\beta_{d1}$, α_{g2}/X_{g2}, $1/\beta_{g2}$ and $X_{g2}f_{g2}$ [calculated from Eq. (9)] into Eq. (8). From the result of analysis we know that the system deforms with three kinds of flow units, two are grain boundary flow units connected in parallel with each other and the other is the dislocational flow units connected in series with the former system. Al-bronze is known as a superplastic material at 800°C.

6. **Zirconium and Zircaloy-2.** Bernstein[10] studied the creep behavior for pure zirconium and zircaloy-2 (Zr base, Sn 1.42%, Fe 0.14%, Cr 0.1%, other metals in trace). The size of the flat specimens was $1\times0.25\times0.02$ in., and the grain size was about 50μ for zirconium and about 10μ for zircaloy-2. The experimental results showed that two mechanisms are rate controlling, one is predominant in the low-stress region where the rate-controlling process is characterized by a grain boundary diffusion creep, and the other is predominant in the higher-stress region where the rate-controlling process is characterized by dislocation movement.

The plot of f *vs.* $-\ln\dot{s}$ of experimental data obtained by Bernstein[10] are shown in *Fig.* 5. The theoretical curves in the figure were obtained by introducing the parameters of zirconium and zircaloy-2 in *Table* 2 into Eq. (6) for Case 3 where a single kind of dislocation flow units and a single kind of grain boundary flow units are connected in series.

7. **Single Crystals.** Since no grain boundaries are present in the interior of single crystals, the creep deformation due to grain boundary flow units will not occur in this case. Thus the creep deformation of single crystals is due to dislocation flow units only. But there will be two cases, in one of which only a single kind of dislocation flow units appears in the deformation whereas in the other a parallel connection of two or more kinds of flow units appear. Creep behavior of single crystals of metals, alloys, ceramics and ionic compounds are considered in the following.

Single crystals of metals, such as Al,[11] Zn,[12] Pb,[13] Ni,[14] all showed the plastic deformation where a single kind of dislocation flow units is acting (Case 1). The theoretical curves of f *vs.* $-\ln\dot{s}$ for these metals are obtained from

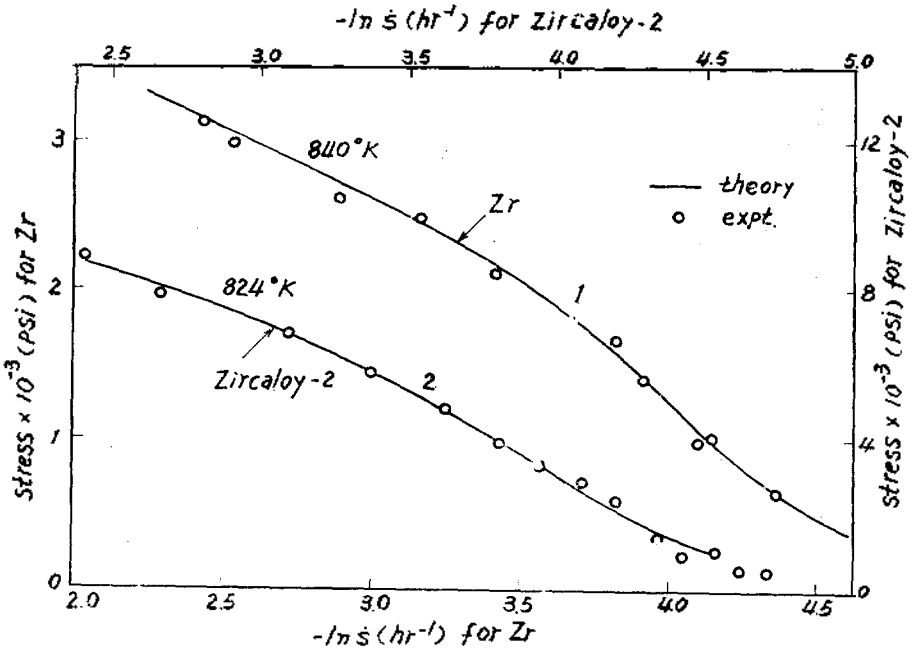

Fig. 5. Creep curves for zirconium of 50μ grain size (curve 1) and zircaloy-2 of about 10μ grain size (curve 2).

Table 3. Flow parameters for single crystals of metals and alloys.

Samples	$\alpha_{\beta 1}$	$1/\beta_{\beta 1}$	Temp. (°K)	*Figure*
Al	2.5×10^{-4} (psi)$^{-1}$	9.97×10^{3} sec^{-1}	10 to 70	*Fig.* 6
Ni	2.33 (kg/mm^2)$^{-1}$	3.97×10^{-5} sec^{-1}	295	*Fig.* 6
Zn	3.36 (g/mm^2)$^{-1}$	1.46×10^{-15} sec^{-1}	546	*Fig.* 6
Pb	1.02×10^{-2} (psi)$^{-1}$	1.82×10^{-3} hr^{-1}	rm. temp.	*Fig.* 6
Ni-Cr (21.5%)	2.32 (kg/mm^2)$^{-1}$	4.42×10^{-14} sec^{-1}	295	*Fig.* 7
Ni-Cr (4.36%)	1.61 (kg/mm^2)$^{-1}$	1.07×10^{-5} sec^{-1}	295	*Fig.* 7
Ni-Cr (21.5%)	1.45 (kg/mm^2)$^{-1}$	6.45×10^{-8} sec^{-1}	550	*Fig.* 7

Eq. (3a) by using the parameters given in *Table* 3. The results are shown in *Fig.* 6, the agreement between theory and experiment is very good.

The results for single crystals of Ni-Cr alloys[14] (Ni base, Cr 4.36% or 21.6%) are shown in *Fig.* 7, all showed plastic deformation due to a single kind of flow units (Case 1). The theoretical curves calculated from Eq. (3a) by using the parameters shown in *Table* 3 are compared with experiment in *Fig.* 7.

Chang[15] examined the creep behavior of single crystals of Al_2O_3 (ruby and sapphire) at 1823°K. Chang explained the experimental result by assuming the mechanism of dislocational climbing-up. But our theoretical curves were obtained by introducing the parameters in *Table* 4 into Eq. (3a) (Case 1), they are in good agreement with experiment as shown in *Fig.* 8.

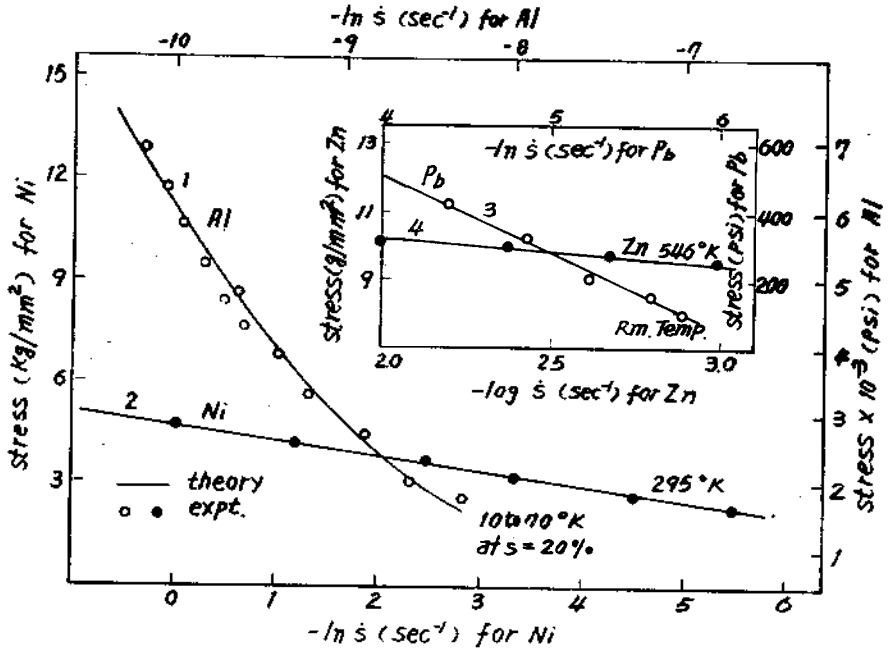

Fig. 6. Creep curves for single crystals of metals. Curve 1, Al; curve 2, Ni; curve 3, Pb; curve 4, Zn.

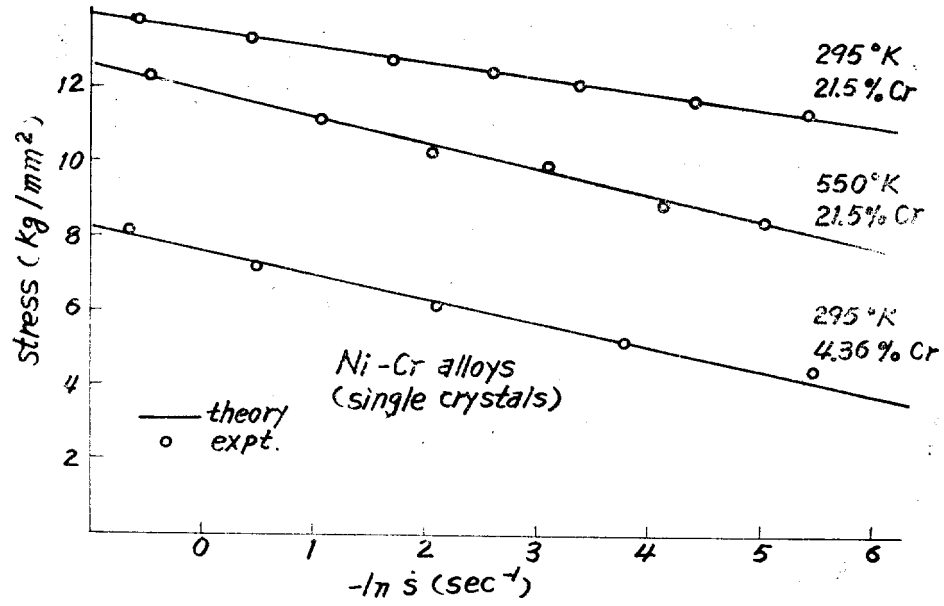

Fig. 7. Creep curves for single crystals of Ni-Cr alloys.

Table 4. Flow parameters for single crystals of oxides and ionic compounds.

Samples	α_{d1}	$1/\beta_{d1}$	Temp. (°C)	*Figure*
Ruby	2.74×10^{-8} (dynes/cm^2)$^{-1}$	7.35×10^{-9} sec^{-1}	1550	*Fig.* 8
Sapphire	6.11×10^{-8} (dynes/cm^2)$^{-1}$	1.46×10^{-8} sec^{-1}	1550	*Fig.* 8
MgO[a]	2.78×10^{-3} g^{-1}	7.61×10^{-9} sec^{-1}[b]	1454	*Fig.* 9
MgO[a]	2.78×10^{-3} g^{-1}	2.63×10^{-8} sec^{-1}[b]	1503	*Fig.* 9
MgO[a]	2.78×10^{-3} g^{-1}	8.28×10^{-8} sec^{-1}[b]	1551	*Fig.* 9
MgO[a]	2.78×10^{-3} g^{-1}	2.81×10^{-7} sec^{-1}	1605	*Fig.* 9
MgO[a]	2.78×10^{-3} g^{-1}	8.37×10^{-7} sec^{-1}[b]	1656	*Fig.* 9
MgO[a]	2.78×10^{-3} g^{-1}	2.22×10^{-6} sec^{-1}[b]	1704	*Fig.* 9
NaCl	1.18×10^{-1} (g/mm^2)$^{-1}$	2.17×10^{-3} sec^{-1}	780	*Fig.* 10
KCl	1.24 (g/mm^2)$^{-1}$	5.77×10^{-18} sec^{-1}	780	*Fig.* 10
LiCl	3.45×10^{-2} (g/mm^2)$^{-1}$[c] 5.91×10^{-2} (g/mm^2)$^{-1}$[d]	2.22×10^{-5} sec^{-1} 2.52×10^{-6} sec^{-1}[e]	780	*Fig.* 10

[a]The unit of the stress was expressed in grams and dimension of the sample was not specified in the original; [b]Values obtained by introducing ΔH_{d1}^{*} (*Table* 5) to Eq. (15a) in reference 1; [c]This value represents α_{d1}/X_{d1}; [d]This value represents α_{d2}/X_{d2}; [e]This value represents $1/\beta_{d2}$.

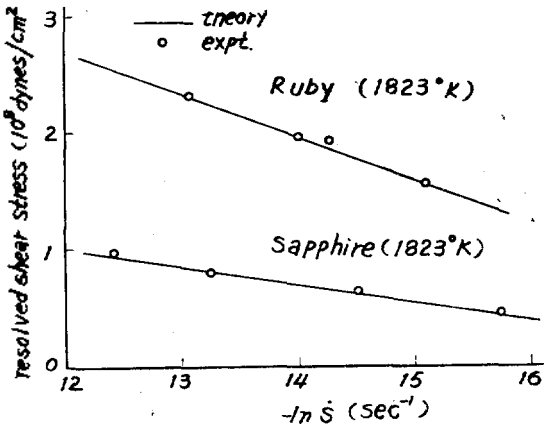

Fig. 8. Creep curves for alumina single crystals (ruby and sapphire).

Cummerow[16] investigated the creep behavior of single crystals of MgO in the temperature range from 1400°C to 1700°C. The MgO single crystals also showed the deformation by a single kind of flow units (Case 1) as shown in *Fig.* 9. The parameters are given in *Table* 4, and the theoretical curves are obtained by using these parameters from Eq. (3a). All the parametric values of $1/\beta_{d1}$ at various temperatures, which were used for calculating the theoretical curves, are the predicted values from the $1/\beta_{d1}$ at 1605°C and ΔH_{d1}^{*} (*Table* 5).

The single crystals of ionic compounds such as NaCl, KCl, LiCl[17] showed the plastic deformation by the dislocation movement as shown in *Fig.* 10. NaCl and KCl showed the flow behavior of Case 1 caused by a single kind of flow units. On the other hand, LiCl single crystals showed the deformation of Case 2, where two kinds of dislocation flow units connected in parallel with each other. The theoretical curves for NaCl and KCl were obtained from Eq. (3a), and the curve for LiCl was obtained from Eq. (4c), in which k is replaced by d, by using the parameters α_{di}/X_{di} and $1/\beta_{di}$ (i=1 or 2) in *Table* 4.

DISCUSSIONS

Activation Enthalpies for Flow Mechanisms. We have assumed that, in plastic deformation of solids, the self-diffusion of the neighboring atoms around bad sites on the slip

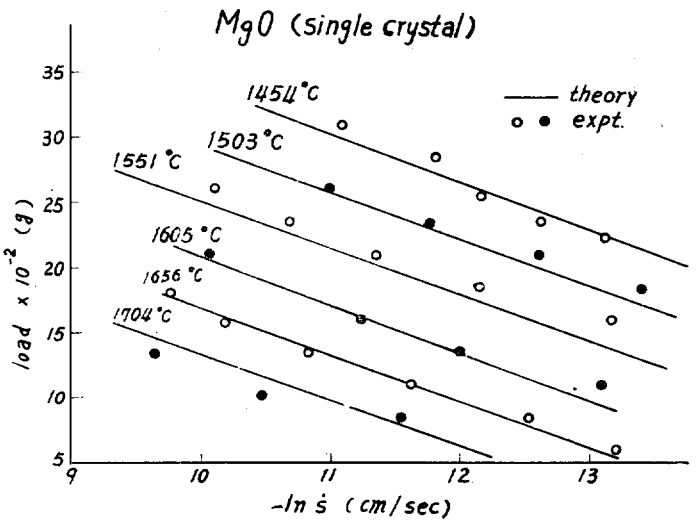

Fig. 9. Creep curves for single crystals of MgO at different temperatures. All the curves except for 1605°C were obtained from the flow parameters at 1605°C (*Table* 4) and ΔH_{d1}^{*} (Table 5).

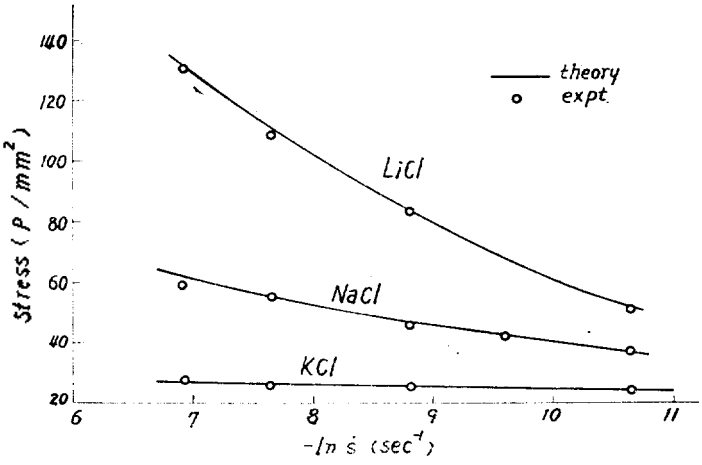

Fig. 10. Creep curves for single crystals of LiCl, NaCl, and KCl.

planes is the rate determining step. Thus the activation enthalpy for plastic deformation may be expected to be equal to that for self diffusion. Since the grain boundary is a region where atoms are distributed randomly with many vacancies, it is also expected that the activation enthalpy (ΔH^{*}_{g1}) for grain boundary movement would be smaller than that (ΔH^{*}_{d1}) for dislocation movement. The quantities, ΔH^{*}_{d1} and ΔH^{*}_{g1}, which were calculated by using the method described in Paper 1 [cf. Eq. (16) of the latter], are presented in *Table* 5, and are compared with the experimental values in the literature. In *Table* 5, the values of ΔH^{*}_{d1} which were indirectly obtained by using Eq. (17) of Paper 1, are also presented; the parenthesized ΔH^{*}_{d1} data in *Table* 5 are the values obtained indrectly.

First, let us consider the result of MgO polycrystals. Referring to *Table* 5, our activation enthalpy for grain boundary movement (ΔH^{*}_{g1}) is 112 kcal/mole, and that for dislocation movement is 160 kcal/mole. The activation enthalpy for self-diffusion of oxygen in MgO single crystals was measured by Cummerow[16] to be 160 kcal/mole, which is in good agreement with our value of ΔH^{*}_{d1}. Our result of grain boundary movement (ΔH^{*}_{g1}=112 kcal/mole) is also in good agreement with the 110 kcal/mole of Hensler.[3] We see here that $\Delta H^{*}_{d1} > \Delta H^{*}_{g1}$ as was predicted previously.

Next, consider the case for ZrO_2. Evans[6] obtained the activation enthalpies of deformation of YSZ at the stress of 4860 psi, the value was 86 kcal/mole. Referring to *Fig.* 2 the stress of 4860 psi is in the range where the deformation by grain boundary movement contributes predominantly. So on the assumption

Table 5. ΔH_{d1}^{*} values for flow mechanisms.[a]

Samples	ΔH_{d1}^{*} (kcal/mole)	ΔH_{g1}^{*} (kcal/mole)	Reference
MgO (polycrystal)	160	112	This work
MgO (single crystal)	[160]		Cummerow[16]
MgO (polycrystal)		110	Hensler[3]
ZrO_2: YSZ	(93)		This work
YSZ		86	Evans[5]
CSZ	[92.5]		Rhodes[18]
Al_2O_3 (polycrystal)	160	114	This work
Al_2O_3 (polycrystal)		130	Folweiler,[7] Warshaw[6]
Al_2O_3 (polycrystal)		[110]	Oishi[19]
Al_2O_3 (single crystal)	[152±5]		Oishi[19]
Al-Zn-Mg-Cu alloy (7075 aluminum)	41	23	This work
Zr metal	(36.1)		This work
Zr metal	~56	29.7	Bernstein[10]
Zr metal	[45.5]		Kidson[20]
Zircaloy-2	(52.1)		This work
Zircaloy-2	68.5	42.5	Bernstein[10]
Zircaloy-2	[~62]		Kidson[20]

[a]Parenthesized data were indirectly obtained from the value of ΔH_{g1}, and square bracketed ones from self-diffusion experiment.

that ΔH_{g1}^{*}=86 kcal/mole, the activation enthalpy for the dislocation movement is calculated to be ΔH_{d1}^{*}=93 kcal/mole by using the indirect method in Paper 1 (*Table* 5). Rhodes and Carter[18] measured the activation enthalpy for the diffusion of Zr^{4+} in the calcia stabilized zirconia (CSZ), and the value was found to be 92.5 kcal/mole. This result is nearly equal to our value of ΔH_{d1}^{*} (=93 kcal/mole), so the deformation by dislocation movement is considered to be controlled by the bulk diffusion of Zr^{4+}.

Next, the case for Al_2O_3 crystals is considered below. Referring to *Table* 5, our values are: ΔH_{g1}^{*}=114 and ΔH_{d1}^{*}=160 kcal/mole. The activation enthalpy found by Folweiler[7] and Warshaw and Norton[6] was ΔH_{g1}^{*}=130 kcal/mole, and the activation enthalpy of O^{18} self-diffusion in polycrystalline alumina (20~30 μ) was 110 kcal/mole (Oishi and Kingery[19]). These experimental values are in good agreement with our value of ΔH_{g1}^{*}=114 kcal/mole. Oishi and Kingery[19] also experimented the O^{18} self-diffusion in single crystals of alumina, and reported the activation enthalpy of 152±5 kcal/mole. This is also in good agreement with our value ΔH_{d1}^{*}=160 kcal/mole.

Now, let us turn to the case of metals and alloys. For the Al-Zn-Mg-Cu alloy, our values, ΔH_{g1}^{*}=23 and ΔH_{d1}^{*}=41 kcal/mole, are presented in *Table* 5. No values of ΔH_{g1}^{*} and ΔH_{d1}^{*} for this alloy have been published on the literature.

Bernstein *et al.*[10] measured the activation enthalpies of zirconium at the stress of 1500 psi, and obtained 29.7 kcal/mole, but at a high stress not specified, the ΔH^{*} value was about 56 kcal/mole. On the assumption of ΔH_{g1}^{*}=29.7 kcal/mole, we calculated ΔH_{d1}^{*}=36.1 kcal/mole by applying the indirect method of Paper 1. Meanwhile the tracer experiment[20] showed ΔH_{d1}^{*}=45.5 kcal/mole. The consider-

able difference between the literature value of ΔH_{s1}^{*} and that of our theory (36.1 kcal/mole) may be due to some erroneous assumption on the value of ΔH_{s1}^{*} (=29.7 kcal/mole.) Referring to *Fig.* 5, the stress of 1500 psi, where ΔH_{s1}^{*} (=29.7 kcal/mole) was obtained, is in the middle range that two mechanisms act considerably mixed. So ΔH_{s1}^{*}=29.7 kcal/mole obtained at this stress may have a considerable error.

For zircaloy-2, Bernstein[10] obtained ΔH_{s1}^{*}= 42.5 kcal/mole at the stress of 1815 psi and ΔH_{s1}^{*}=68.5 kcal/mole at higher stresses. Our ΔH_{s1}^{*} value of 52.1 kcal/mole was calculated by using the indirect method under the assumption that ΔH_{s1}^{*}=42.5 kcal/mole. According to the tracer experiment,[20] ΔH_{s1}^{*} is about 62 kcal/mole for Zr-1.3% Sn alloy. In *Fig.* 5, the stress of 1815 psi is in the range where the deformation by grain boundary movement is predominantly occurring, so the assumption that ΔH_{s1}^{*}=42.5 kcal/mole is considered to be valid. Using this assumption, the value of ΔH_{s1}^{*}=52.1 kcal/mole was obtained by the indirect method. This value is much smaller than the experimental values of 62 and 68.5 kcal/mole. Taking into account of the approximation introduced in the determination of ΔH_{s1}^{*}, however, the result may be said to be satisfactory.

ACKNOWLEDGMENT

This research was supported by the Euisok Research Foundation. We express our sincere thanks for the financial assistance.

REFERENCES

1. C.H. Kim and T. Ree, *This Journal*, **21**, 330 (1968)
2. H. Eyring, *J. Chem. Phys*, **4**, 283 (1936).
3. J.H. Hensler and G.V. Cullen, *J. Amer. Ceram. Soc.*, **51**, 557 (1968).
4. S. J. Hahn, T. Ree and H. Eyring, *Geol. Soc. Am. Bull.*, **78**, 773 (1967).
5. P.E. Evans, *J. Amer. Ceram.* Soc., **53**, 365 (1970).
6. S.I. Warshaw and F.H. Norton, *J. Amer. Ceram. Soc.*, **45**, 479 (1962).
7. C. Folweiler, *J. Appl. Phys.*, **32**, 773 (1961).
8. J. D. Embury, B.A. Wilcox and A. H. Clauer, *J. Inst. Metals*, **100**, 153 (1972).
9. G. L. Dunlop and D. M. R. Taplin, *J. Mater. Sci.*, **7**, 316 (1972).
10. I. M. Bernstein, *Trans, Metall. Soc. AIME*, **239**, 1518 (1967).
11. A. Kumar, F. E. Hauser and J. E. Hauser and J. E. Dorn, *Acta Met.*, **16**, 1189 (1968).
12. J. J. Gilman, *J. Metals*, **8**, 1326 (1956).
13. R.C. Gifkins and K.U. Snowden, *Trans. Metall. Soc. AIME*, **239**, 910 (1967).
14. A. Akhtar and E. Teghtsoonian, *Met. Trans*, **2**, 2757 (1971).
15. R. Chang, *J. Appl. Phys.*, **31**, 484 (1960).
16. R.L. Cummerow, *J. Appl. Phys.*, **34**, 1724 (1963).
17. S. N. Comnik, V. Z. Bengus and E. D. Lyak, *Phys. Status Solidi.*, **19**, 533 (1967).
18. W.H. Rhodes and R.E. Carter, *J. Amer. Ceram. Soc.*, **49**, 244 (1966).
19. Y. Oishi and W. D. Kingery, *J. Chem. Phys.*, **33**, 480 (1960).
20. C.V. Kidson, *Electrohem. Tech.*, **4**, 193 (1966).